DOI: 10.1002/ejic.200900743

Structural and Photophysical Properties of (Phosphane)gold(I)-Decorated 4,4′-Diethynyl-2,2′-bipyridine Ligands

Edwin C. Constable,*[a] Catherine E. Housecroft,*[a] Marzena K. Kocik,[a] Markus Neuburger,[a] Silvia Schaffner,[a] and Jennifer A. Zampese[a]

Keywords: Gold / Heterocycles / Alkynes / 2,2′-Bipyridine / Phosphane ligands / Photophysics

Treatment of 4,4′-diethynyl-2,2′-bipyridine with R_3PAuCl (R = Ph, 4-Tol, Et, *i*Pr) leads to the formation of a family of (phosphane)gold(I)-decorated 4,4′-diethynyl-2,2′-bipyridine ligands. The solid-state structures of the compounds are significantly affected by the change from aryl- to alkyl-substituted phosphanes, whereas the progression from ethyl to isopropyl substituents leads to a subtle change in the packing that results in the propagation of two different polymeric chain motifs, both supported by close Au···Au contacts [3.1239(1) Å for R = Et, and 3.395(1) Å for R = *i*Pr]. In CH_2Cl_2 solution, each of the compounds **1**–**4** is a dual emitter at room temperature. When the excitation wavelength is approximately 238 nm, the emission spectra of **1** and **2** exhibit new bands at 288 and 570 nm at the expense of the original emissions. The photodegradation is not inconsistent with the formation of gold nanoclusters.

Introduction

The formation of Au–C σ-bonds by coupling terminal alkynes with Au^I centres is well established.[1,2] Interest in gold(I)-containing compounds arises from their potential applications in advanced materials, largely because of their luminescent properties.[3–7] Among the first photoemissive alkynylgold(I) complexes to be described in the literature were $Ph_3PAuC{\equiv}CPh$ and $\{PhC{\equiv}CAu\}_2(\mu\text{-dppe})$ (dppe = $Ph_2PCH_2CH_2PPh_2$). Che and co-workers[8] showed that these species possess long-lived and emissive excited states in CH_2Cl_2 solution at ambient temperature, and upon going from solution to the solid state, a dramatic redshift in the emission maximum of $\{PhC{\equiv}CAu\}_2(\mu\text{-dppe})$ was observed. The presence of short (approximately 3.00–3.20 Å) Au···Au contacts in the solid state is thought to be fundamental to emissive behaviour.[3,9–11]

By combining phosphane and alkyne metal-binding domains at a gold(I) centre, one gains a significant scope for the design of macromolecules:[12] rigid-rod P–Au–C≡C– domains and a wide range of readily accessible mono-, bi- and polydentate phosphane ligands containing sp^3-hybridized P atoms combine with a tendency for gold atoms to aggregate (so-called "aurophilicity").[13–16] Of the 215 compounds in the CSD (CSD version 5.3 with May 2009 updates, Conquest version 1.11)[17] possessing $R_3PAuC{\equiv}C$ units, only 19[9,18–32] exhibit intermolecular aurophilic interactions resulting in one-dimensional Au···Au bonded polymers. Of particular relevance to our work is the trigold derivative $(n\text{Bu}_3\text{PAuC}{\equiv}\text{CCH}_2\text{OCH}_2)_3\text{CCH}_2\text{Otpy}$ (tpy = 2,2′:6′,2"-terpyridine), which forms one-dimensional chains with an oriented assembly in the solid state in which all the tpy units point in the same direction.[19] The incorporation into alkynylgold(I)-containing assemblies of additional metal-binding domains such as tpy,[19,30,33] bpy[30,32,34–37] (bpy = 2,2′-bipyridine) or 1,10-phenanthroline[38] allows the incorporation of redox- or photoactive metal centres for tuning (or switching if metal-binding is reversible) the physical properties of the material. For enhancing the emission properties, molecular-design considerations need to take into account the steric demands of the gold(I) substituents so that aurophilic interactions may be optimized. It should be noted, however, that even though close gold–gold contacts may appear to be accessible in the solid state, competition with hydrogen-bonding and other weak interactions may dominate in the packing.[33] In contrast, aurophilic and hydrogen-bonded interactions[39] or metal binding[40] may act in a cooperative manner.

At a separation of approximately 3 Å, the strength of an attractive Au···Au interaction is about 30 $kJ\,mol^{-1}$,[41] and this is comparable with the dissociation enthalpy of a classical hydrogen bond.[15]

We report here a series of 2,2′-bipyridine ligands (Scheme 1), decorated in the 4- and 4′-positions with (alkynyl)(phosphane)gold(I) units, and discuss the relationship between their solid-state structures and their solid-state and solution emissive properties.

[a] Department of Chemistry, University of Basel, Spitalstrasse 51, 4056 Basel, Switzerland
Fax: +41-61-267-1008
E-mail: Catherine.Housecroft@unibas.ch

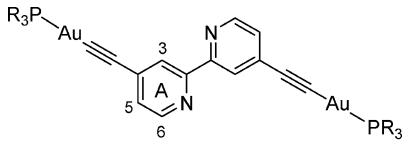

1 R = Ph
2 R = 4-Tol
3 R = Et
4 R = *i*Pr

Scheme 1. Structures of compounds **1**–**4** with the numbering scheme used for NMR spectroscopic assignments; for **1** and **2**, the phenyl ring is labelled B.

Results and Discussion

Synthesis and Solution Characterization

Compounds **1**–**4** (Scheme 1) were prepared by the reaction of 4,4′-diethynyl-2,2′-bipyridine[42] with the appropriate R_3PAuCl in a mixture of toluene, CH_2Cl_2 and diisopropylamine in the presence of CuI.[43] The reactions were monitored by spot thin layer chromatography, and under ambient conditions, the reactions required 12–16 h to reach completion. However, upon heating in THF or CH_2Cl_2 at 50 °C in a microwave reactor, each reaction was complete within 30 min.

The base peak in the electrospray mass spectrum of **1** appeared at *m*/*z* = 1121.8 and corresponds to the $[M + H]^+$ ion. Very low intensity peaks at *m*/*z* = 721.7 (<5%) and 1579.4 (<5%) were assigned to $[Au(Ph_3P)_2]^+$ and $[M + AuPPh_3]^+$. In contrast, the base peak in the ESI mass spectrum of **2** corresponds to $[Au\{(4\text{-Tol})_3P\}_2]^+$ (*m*/*z* = 805.2), and the next most intense peak to $[M + AuP(4\text{-Tol})_3]^+$ [*m*/*z* (%) = 1705.0 (59)]. The $[M + H]^+$ ion was observed only as a low-intensity peak [*m*/*z* (%) = 1205.1 (28)]. This same pattern of peaks was also observed for **3** and **4**, but for these compounds, the base peak corresponds to $[M + AuPEt_3]^+$ (*m*/*z* = 1147.1) or $[M + AuP{i}Pr_3]^+$ (*m*/*z* = 1273.2), and the $[M + H]^+$ peak was observed with relative abundances of 10 and 3%, respectively.

The ^1H and ^{13}C NMR spectra of the compounds are in accord with the symmetrical structure shown in Scheme 1. However, it was not possible to resolve signals in any of the ^{13}C NMR spectra for the alkyne carbon atoms. The ^{31}P NMR spectrum of each compound exhibits one signal, shifted from that of the corresponding R_3PAuCl. The solution electronic absorption and emission data are discussed later in this paper.

Structural Determinations

Crystals of $2\{\mathbf{1}\}\cdot Et_2O$ and $\mathbf{2}\cdot Et_2O$ suitable for single X-ray diffraction were grown by slow diffusion of Et_2O into a CH_2Cl_2 solution of **1**, or a toluene/CH_2Cl_2 solution of **2**. The structures of the compounds are shown in Figures 1 and 2, respectively. Whereas **2** is centrosymmetric, **1** contains two independent gold atoms. The bpy unit in both derivatives adopts the expected *transoid* conformation, with the angle between the least-squares planes of the two pyridine rings being 8.8(3)° in **1** and constrained by symmetry to 0° in **2**. The environment around the P atoms is unexceptional, with P–C bond lengths in **1** and **2** lying in the ranges 1.790(5)–1.825(6), and 1.812(1)–1.816(1) Å, respectively. There is only a small deviation from linearity along the P–Au–C≡C–C_{bpy} units, with the smallest angle subtended at any of the gold and alkyne carbon atoms being 174.6(2)° at Au2 in **1**, and 176.83(5)° at Au1 in **2**. In both $2\{\mathbf{1}\}\cdot Et_2O$ and $\mathbf{2}\cdot Et_2O$, the diethyl ether molecules are disordered. The Et_2O molecule was modelled over two positions in each compound; in $\mathbf{2}\cdot Et_2O$, the O atom was common to both positions. The centrosymmetric pair of molecules of **1** in the unit cell engage in edge-to-face interactions between phenyl rings. Figure 3 highlights these interactions and also shows how the alkyne carbon atoms C32 and C33 form close contacts to a CH unit of a phenyl ring on an adjacent molecule. The C31C32 alkyne unit also interacts with a phenyl ring of another molecule of **1** [C32···H361^{iii} 2.88, C32···C36^{iii} 3.435(9) Å; symmetry code iii = 1 + *x*, *y*, *z*]. In $\mathbf{2}\cdot Et_2O$,

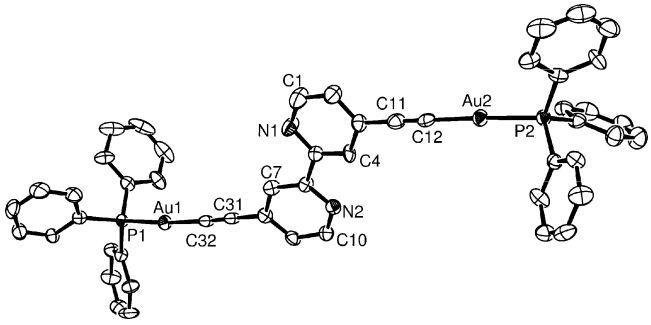

Figure 1. Molecular structure of compound **1** in $2\{\mathbf{1}\}\cdot Et_2O$ (ellipsoids plotted at the 50% probability level). Selected bond lengths [Å] and angles [°]: Au1–P1 2.263(1), Au1–C32 2.000(6), Au2–P2 2.271(1), Au2–C12 2.015(7), C11–C12 1.160(9), C31–C32 1.184(8); P1–Au1–C32 174.6(2), P2–Au2–C12 177.7(2), C3–C11–C12 179.4(7), Au2–C12–C11 179.6(6), C8–C31–C32 176.4(6), C31–C32–Au1 175.7(5).

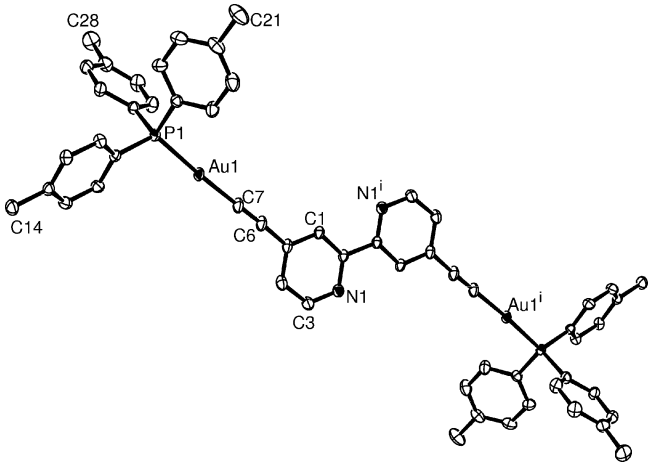

Figure 2. Molecular structure of compound **2** (ellipsoids plotted at the 50% probability level) in $\mathbf{2}\cdot Et_2O$. Selected bond lengths [Å] and angles [°]: Au1–P1 2.2802(3), Au1–C7 1.997(1), C6–C7 1.213(2); P1–Au1–C7 176.83(5), C5–C6–C7 177.1(2), C6–C7–Au1 178.9(2). Symmetry code: i = –*x*, –*y*, –*z*.

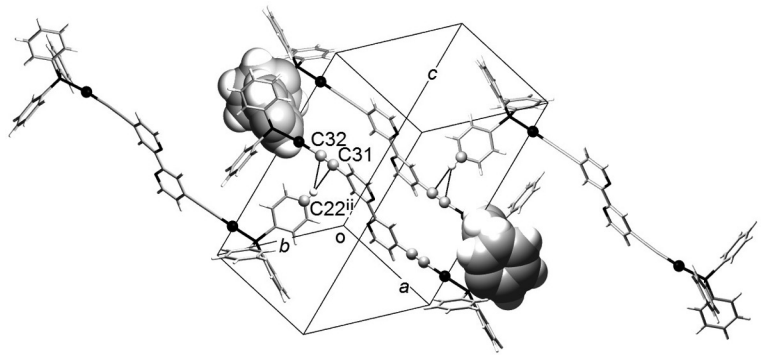

Figure 3. Packing of molecules of **1**: (i) edge-to-face interactions between symmetry-related molecules in the unit cell are shown in space-filling representation (C48–H481···centroid to ring containing C19^{i} 2.54 Å; C48–H481···centroid 166°; symmetry code i = 1 – *x*, 1 – *y*, 1 – *z*), and (ii) aromatic CH···alkyne interactions [C32···H221^{i} 2.80, C32···C22^{i} 3.574(9), C33···H221^{ii} 2.72, C33···C22^{i} 3.582(9) Å; symmetry code ii = –1 + *x*, 1 + *y*, *z*]. Au (ball representation), N and P atoms (stick representation) are shown in black.

similar close contacts are observed between molecules of **2**, but this time involving the methyl group of one tolyl substituent [C7···H212^{ii} 2.85 Å, C7···C21^{ii} 3.764(3) Å; symmetry code ii = –1 + *x*, *y*, *z*]. Packing motifs based on C–H···C_{alkyne} contacts are well established in the solid-state structures of alkynes with aromatic substituents,[44–49] and C–H···C_{alkyne} interactions are ubiquitous among compounds containing $R_3PAuC{\equiv}C$ units (CSD version 5.3 with May 2009 updates, Conquest version 1.11),[17] involving both aromatic and aliphatic C–H units. There are no significant intermolecular Au···Au contacts in either **1** or **2**, the closest separations being Au2···Au2^{i} 4.763(1) Å in **1** (symmetry code i = 2 – *x*, –*y*, –*z*), and Au1···Au1^{iii} 5.303(1) Å in **2** (symmetry code iii = 1 – *x*, 1 – *y*, –*z*). In the light of the structure of compound **4** (see below), the lack of Au···Au interactions cannot simply be attributed to the steric demands of the triarylphosphane units [Tolman cone angles for PPh_3 and $P(4\text{-Tol})_3$: 145°].[50]

Single crystals of **3** and **4** were grown by slow diffusion of Et_2O into a CH_2Cl_2 solution of each compound. Figures 4 and 5 depict the molecular structures and give selected bond parameters. In the triethylphosphane derivative **3**, the gold atoms are in independent (but chemically similar) environments, whereas the triisopropylphosphane derivative **4** is centrosymmetric. In **4**, one of the isopropyl groups is disordered and has been modelled over two sites of fractional occupancies 0.64 and 0.36. The backbone of each of **3** and **4** is significantly more bowed than those in **1** and **2**, with the smallest angles subtended at the gold or alkyne carbon atoms being 166.7(2)° at C14 in **3**, and 172.8(3)° at Au1 in **4**. The bpy unit is constrained by symmetry to planarity in **4**, and in **3**, the angle between the least-squares planes of the two pyridine rings is 11.3(1)°. Figure 6 illustrates that there are clear similarities in the

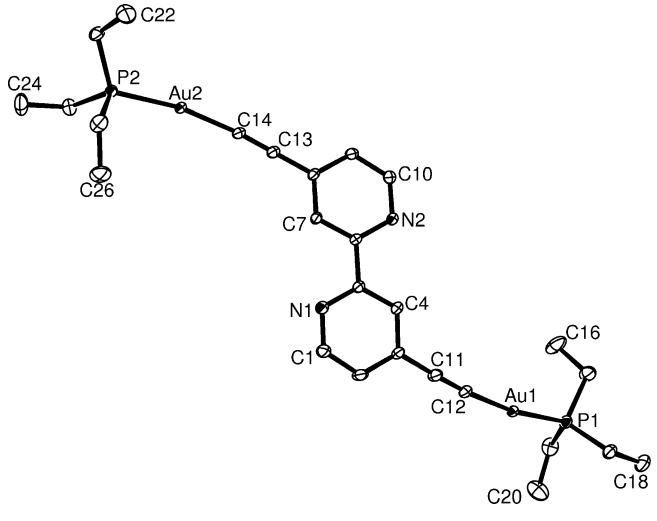

Figure 4. Molecular structure of compound **3** (thermal ellipsoids plotted at 50% probability level). Selected bond lengths [Å] and angles [°]: Au1–P1 2.2808(6), Au1–C12 2.004(2), Au2–P2 2.2801(6), Au2–C14 1.999(2), C11–C12 1.213(3), C13–C14 1.216(3); P1–Au1–C12 170.77(7), P2–Au2–C14 167.52(7), C3–C11–C12 173.2(3), C11–C12–Au1 171.2(2), C8–C13–C14 176.6(3), C13–C14–Au2 166.7(2).

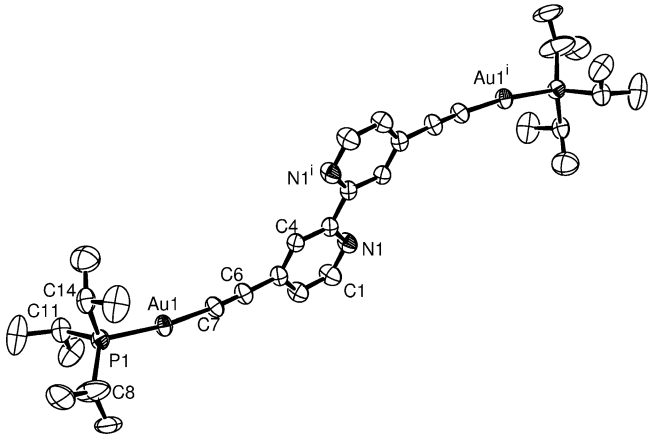

Figure 5. Molecular structure of compound **4** (ellipsoids plotted at the 40% probability level). Selected bond lengths [Å] and angles [°]: Au1–P1 2.282(2), Au1–C7 1.996(8), C6–C7 1.19(1); C7–Au1–P1 172.8(3), C7–C6–C3 175.0(9), C6–C7–Au1 175.5(8)°. Symmetry code i = –*x*, –*y*, –*z*. The *i*Pr group containing atom C8 is disordered; only the major occupancy position is shown.

overall packing of **3** and **4**, with weak interactions between alkyl C–H groups and the bpy domains of adjacent molecules, as well C–H_{alkyl}···C_{alkyne} contacts (Table 1).

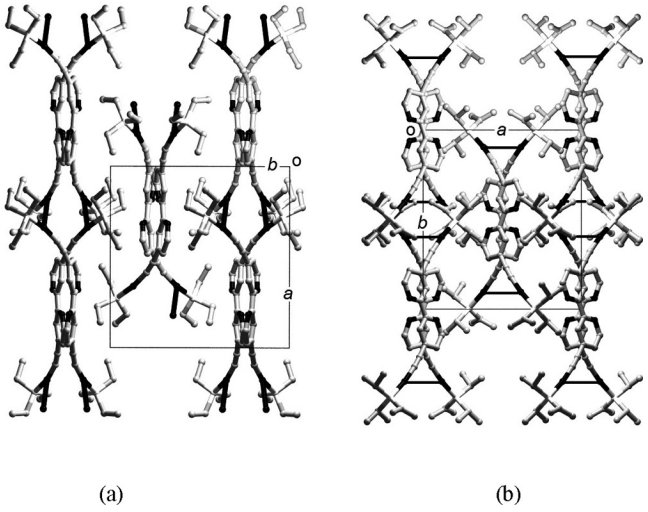

(a) (b)

Figure 6. Packing of molecules of (a) **3** and (b) **4**. Au···Au contacts in each chain are shown in black. Each unit cell is viewed directly along the crystallographic *c*-axis.

Table 1. C–H···N non-classical hydrogen bonds and C–H···C_{alkyne} interactions in **3** and **4**.

D–H···A [Å]	H···A [Å]	D···A [°]	D–H···A	Symmetry codes a–e
3				
C19–H191···N2[a]	2.66	3.617(4)	171	1 – *x*, 1/2 + *y*, 3/2 – *z*
C25–H252···N1[b]	2.79	3.717(4)	159	–*x*, 1 – *y*, –*z*
C23–H231···C14[c]	2.88	3.659(4)	144	*x*, 3/2 – *y*, –1/2 + *z*
4				
C11–H11A···N1[d]	2.88	3.84(1)	161	1/2 + *x*, 1/2 – *y*, 1 – *z*
C10–H10B···C6[e][a]	2.95	3.90(3)	163	*x*, –*y*, –1/2 + *z*
C10–H10B···C7[e][a]	2.94	3.78(3)	143	*x*, –*y*, –1/2 + *z*

[a] H10B is the major occupancy site for the disordered H atom; the site for the minor occupancy H10D also permits a comparable C–H···C interaction.

In contrast to the situation in 2{**1**}·Et_2O and **2**·Et_2O, the gold atoms in **3** and **4** approach each other closely. In **3**, the Au1···Au2^i separation is 3.1239(1) Å (Figure 7), and in **4**, Au1···Au1^{ii} is 3.395(1) Å (symmetry code ii = 1 – *x*, *y*, 1/2 – *z*). These close contacts lead to the assembly of polymeric chains. However, careful inspection of Figure 6 (in which the Au···Au contacts in each chain are shown as black lines) shows that the directions in which the infinite chains are propagated are significantly different. This is quantified in the noticeable difference between the C_{alkyne}–Au···Au–C_{alkyne} dihedral angles in **3** and **4**. In **4**, C7–Au1···Au^{ii}–C7^{ii} is 101.5° (symmetry code ii = 1 – *x*, *y*, 1/2 – *z*), whereas in **3**, the dihedral angle C12–Au1···Au2^i–C14^i is –127.8° (symmetry code i = 1 + *x*, 3/2 – *y*, 1/2 + *z*). We propose that the primary intermolecular interactions controlling the overall assembly are weak hydrogen bonds and C–H···π and van der Waals interactions. In each solid-state structure, each gold atom has two neighbouring gold atoms, one at a separation of <3.4 Å and a second at just over twice this distance (7.389 Å in **3** and 8.654 Å in **4**). The difference in the Tolman cone angle of the phosphane (PEt_3 132° and P*i*Pr_3 160°),[50] appears to be sufficient to tune the packing so that the dominant aurophilic interactions are between spatially distinct pairs of gold atoms resulting in the different chain assemblies shown in Figure 7.

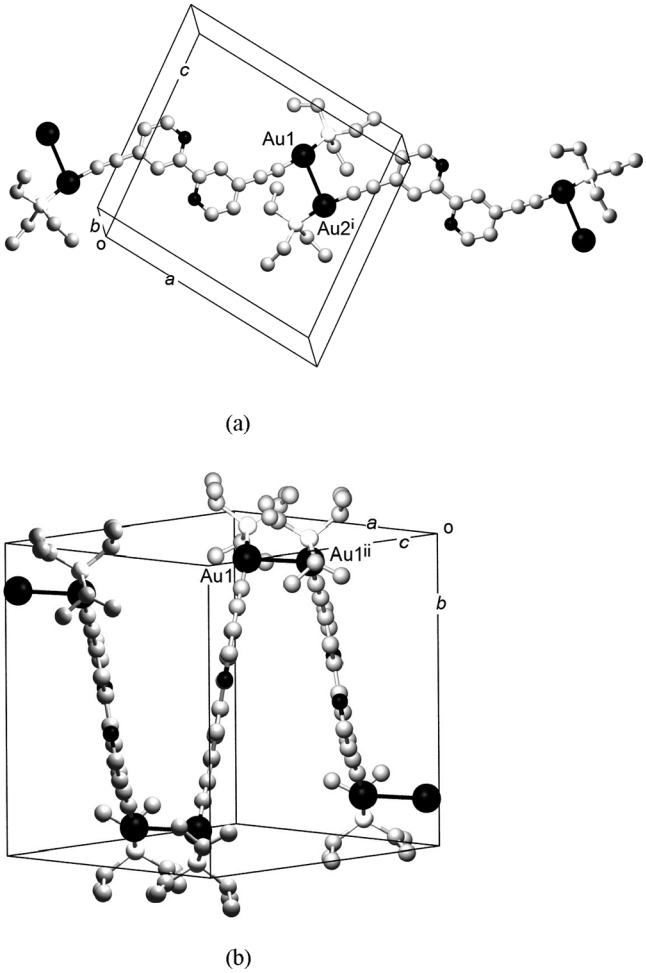

(a)

(b)

Figure 7. Molecules of (a) **3** and (b) **4** form chains by virtue of short Au···Au contacts. **3**: Au1···Au2^i 3.1239(1) Å (symmetry code: i = 1 + *x*, 3/2 – *y*, 1/2 + *z*); **4**: Au1···Au1^{ii} 3.395(1) Å (symmetry code ii = 1 – *x*, *y*, 1/2 – *z*).

Absorption and Emission Properties

The dominant band in the absorption spectrum of a CH_2Cl_2 solution of 4,4′-diethynyl-2,2′-bipyridine is at 233 nm, with lower intensity, overlapping bands at 298 and 310 nm, the latter being redshifted from the absorption at 280 nm in 2,2′-bipyridine[51] (Figure 8). These absorptions arise from alkyne and bpy π*←π and π*←n transitions. Figure 8 also shows the absorption spectra of the free phosphanes Ph_3P[52] and $(4\text{-Tol})_3P$, both of which show absorption maxima at 264 nm. On going from 4,4′-diethynyl-2,2′-bipyridine to compounds **1**–**4**, the highest-energy band in each spectrum lies between 235 and 239 nm and is presumably alkyne-centred (Figures 8 and 9). The more intense ab-

sorptions around 260 nm for compounds **1** and **2** compared to **3** and **4** are attributed to the presence of the aryl substituents in the former. Above approximately 260 nm, there is a common pattern of absorptions across the series of derivatives (Figure 9), and by comparison with related systems,[8,30,31,53,54] we propose that these bands arise from bpy/alkyne π*←π transitions with involvement of Au orbitals.

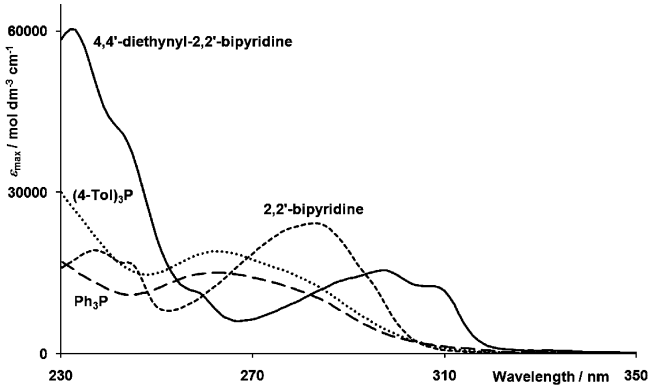

Figure 8. Absorption spectra of CH_2Cl_2 solutions of model compounds bpy, 4,4′-diethynyl-2,2′-bipyridine, Ph_3P and $(4\text{-Tol})_3P$.

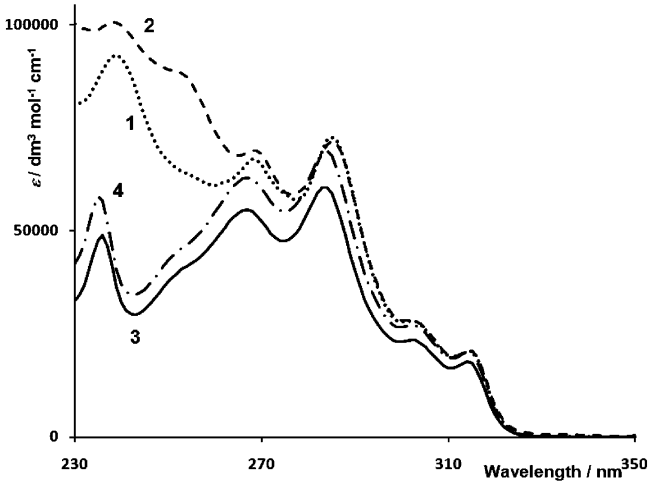

Figure 9. Absorption spectra of compounds **1** (R = Ph), **2** (R = 4-Tol), **3** (R = Et) and **4** (R = *i*Pr) in CH_2Cl_2.

In CH_2Cl_2 solution, each of the compounds **1**–**4** is a dual emitter at room temperature (Figure 10). The general shape of the emission spectra is similar to that reported by Vicente et al. for the (triphenylphosphane)gold(I) derivative of 5-ethynyl-2,2′-bipyridine.[30] Excitation of compound **1** (in CH_2Cl_2) at 239 nm leads to emission bands at 344 and 438 nm, and a well-defined shoulder appears at 466 nm when the compound is excited at 268 or 285 nm, i.e. in the region of the bpy/alkyne-centred absorptions. A similar behaviour is observed for **2**–**4**. For each of the derivatives **1**–**4**, the lower energy emission is the more intense of the two, the reverse of that observed for (2,2′-bipyridine-5-ethynyl)-(triphenylphosphane)gold.[30] Figure 10 shows that the energy and intensity of the emissions are virtually independent of the phosphane substituent. The excitation spectrum of a CH_2Cl_2 solution of **1** shows that each of the emissions at 344, 438 amd 466 nm originates from the broad absorptions between 250 and 320 nm.

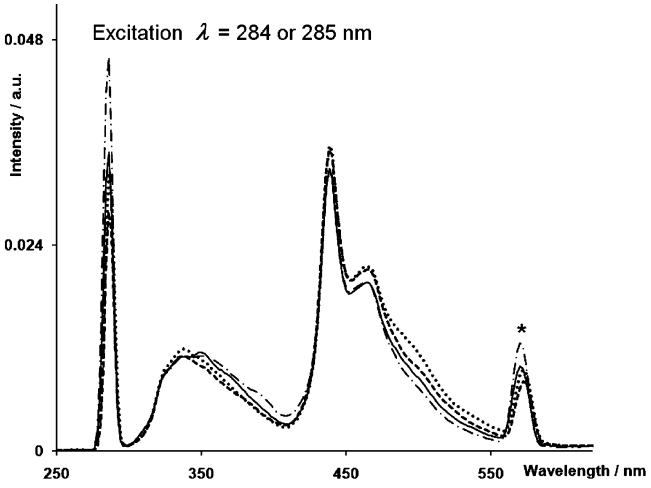

Figure 10. Emission spectra of compounds **1**–**4**; the key for the curves is the same as that in Figure 9. Concentration of each CH_2Cl_2 solution is 1.2×10^{-5} mol dm^{-3} (* = first harmonic).

When sequential solution (CH_2Cl_2) emission spectra of compounds **1** and **2** were recorded over a period of about 30 min (approximately 20–25 spectra), we observed a decay of the bands shown in Figure 10 and a growth of emission bands at 288 and 570 nm (Figure 11) when the excitation wavelength was 238 or 239 nm. No such changes were observed when the compounds were excited at higher wavelengths. Absorption spectra recorded immediately after each series of emission spectra revealed new absorptions at 323 and 366 nm when λ_{exc} had been 238 nm, and no change in the absorption spectra when λ_{exc} had been 253 (for compound **2**), 269 or 286 nm (for compounds **1** and **2**). We have been unable to determine the nature of the photodegradation product, but tentatively propose that it arises from cleavage of the alkynyl–gold bond because the absorption band at approximately 238 nm is most likely to be alkyne-centred. The trialkylphosphane derivatives **3** and **4** behave similarly, although the emissions from the degradation products are very much less intense than from compounds

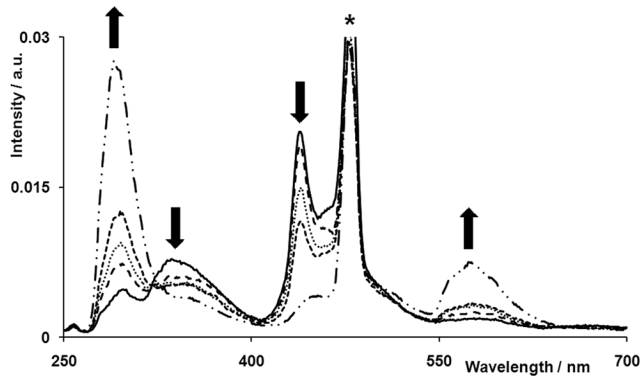

Figure 11. Emission spectrum of a CH_2Cl_2 solution of compound **2** as a function of time (λ_{ex} = 238 nm; * = first harmonic.).

1 and **2**. The observation of the emission at 570 nm upon photodegradation is not inconsistent with the formation of small gold nanoclusters.[55]

Conclusions

We have shown that bis[(phosphane)gold(I)]-decorated 4,4′-diethynyl-2,2′-bipyridine ligands can be readily prepared by reaction of 4,4′-diethynyl-2,2′-bipyridine with R_3PAuCl (R = Ph, 4-Tol, Et, *i*Pr). The solid-state structures of the four compounds (**1**–**4**) show a dependence upon the presence of aryl- or alkyl-substituted phosphane, and the change from ethyl to isopropyl substituents leads to a subtle alteration in the packing that results in the propagation of two different polymeric chain motifs, both supported by close Au···Au contacts [3.1239(1) Å for R = Et, and 3.395(1) Å for R = *i*Pr]. In CH_2Cl_2 solution, each of the compounds **1**–**4** is a dual emitter at room temperature. When the excitation wavelength is approximately 238 nm, the emission spectra of the compounds decay over a period of about 30 min, and for each of **1** and **2**, new bands at 288 and 570 nm become the dominant features of the emission spectrum. The photodegradation is not inconsistent with the formation of gold nanoclusters.

Experimental Section

General: ^1H and ^{13}C NMR spectra were recorded at approximately 295 K with Bruker Avance DRX-500 or DPX-400 MHz spectrometers; for ^1H and ^{13}C, chemical shifts are relative to residual solvent peaks (TMS: δ = 0 ppm) and for ^{31}P relative to external 85% aqueous H_2PO_4. A Shimadzu FTIR-8400S spectrophotometer was used to record IR spectra (solid samples on a Golden Gate diamond ATR accessory). Electrospray ionization (ESI) mass spectra were recorded with Finnigan MAT LCQ or Bruker esquire 3000^{plus} instruments. Electronic absorption and emission spectra were recorded with a Varian-Cary 5000 spectrophotometer and Shimadzu RF-5301 PC spectrofluorometer, respectively. Microwave reactions were performed in a Biotage Initiator 8 reactor. Solvents were distilled before use (water content monitored by Karl-Fischer titration), and all reactions were carried out under N_2. R_3PAuCl (R = Et, *i*Pr, Ph, 4-Tol), were prepared from $HAuCl_4 3H_2O$ (Sigma–Aldrich) according to a published procedure.[56] For Ph_3PAuCl and $(4\text{-Tol})_3PAuCl$, the reactions were carried out at –5 °C; remaining syntheses were carried out at –20 °C. The R_3PAuCl products were purified by washing with hot hexane. Compounds **1**–**4** were prepared according to either Method 1 or 2, with yields being similar for either route for a given phosphane.

Method 1: R_3PAuCl (R = Et, *i*Pr, Ph, 4-Tol), 4,4′-diethynyl-2,2′-bipyridine and CuI were dissolved in a mixture of CH_2Cl_2 (or THF) (6 mL) and toluene (2 mL). Diisopropylamine (predistilled, 2 mL) was added to make the solution basic. The reaction mixture was stirred at room temperature in the dark for 12–16 h, after which time it was filtered and the solvent removed from the filtrate in vacuo. The crude material was purified by preparative plate chromatography in the dark (Al_2O_3, CH_2Cl_2).

Method 2: R_3PAuCl (R = Et, *i*Pr, Ph, 4-Tol), 4,4′-diethynyl-2,2′-bipyridine and CuI were added to argon-degassed THF (or CH_2Cl_2) (8 mL). Diisopropylamine (predistilled, 2 mL) was added to make the solution basic. The reaction mixture was placed in a vial in a microwave reactor (50 °C, 30 min), after which it was filtered and the solvent removed from the filtrate. The crude material was purified by preparative plate chromatography in the dark (Al_2O_3, CH_2Cl_2).

Compound 1: Ph_3PAuCl (126 mg, 255 μmol), 4,4′-diethynyl-2,2′-bipyridine (26 mg, 130 μmol) and CuI (0.2 mg, 1 μmol). Compound **1** was isolated as white solid (97.1 mg, 86.6 μmol, 68.1%). ^1H NMR (500 MHz, $CDCl_3$): δ = 8.51 (d, J = 5.0 Hz, 2 H, H^{A6}), 8.38 (s, 2 H, H^{A3}), 7.51 (m, 18 H, $H^{B3/2+B4}$), 7.44 (m, 12 H, $H^{B2/3}$), 7.30 (dd, J = 5.0, 1.1 Hz, 2 H, H^{A5}) ppm. ^{13}C NMR (126 MHz, $CDCl_3$): δ = 156.1 (C^{A2}), 149.1 (C^{A6}), 134.5 (d, J_{PC} = 14 Hz; $C^{B2/3}$), 134.1 (C^{A4}), 131.8 (C^{B4}), 129.8 (d, J_{PC} = 56 Hz, C^{B1}), 129.5 (d, J_{PC} = 12 Hz, $C^{B2/3}$), 126.4 (C^{A5}), 124.4 (C^{A3}) (C≡C signals not observed) ppm. ^{31}P NMR (162 MHz, $CDCl_3$): δ = 39.0 (s) ppm. UV/Vis (CH_2Cl_2): λ_{max} (ε) = 239 (92500), 269 (67000), 286 (72000), 303 (28000), 315 (21000 $dm^3 mol^{-1} cm^{-1}$) nm; emission (CH_2Cl_2, λ_{exc} = 285 nm): λ_{max} = 338, 438, 466 nm. ESI-MS (CH_2Cl_2): m/z = 1121.8 $[M + H]^+$ (calcd. 1121.2). $C_{50}H_{36}Au_2N_2P_2 \cdot 1.5H_2O$ (1147.74): calcd. C 52.32, H 3.42, N 2.44; found C 52.26, H 3.46, N 2.49.

Compound 2: $(4\text{-Tol})_3PAuCl$ (105 mg, 196 μmol), 4,4′-diethynyl-2,2′-bipyridine (20 mg, 98 μmol) and CuI (0.2 mg, 1 μmol). Compound **2** was isolated as white solid (62.2 mg, 51.6 μmol, 53.4%). ^1H NMR (500 MHz, $CDCl_3$): δ = 8.51 (d, J = 5.0 Hz, 2 H, H^{A6}), 8.37 (s, 2 H, H^{A3}), 7.41 (dd, J_{PH} = 12.5, J_{HH} = 8.0 Hz, 12 H, H^{B3}), 7.30 (dd, J = 5.0, 1.4 Hz, 2 H, H^{A5}); 7.23 (d, J_{PH} = 1.4, J_{HH} = 8.0 Hz, 12 H, H^{B2}), 2.40 (s, 18 H, H^{Me}) ppm. ^{13}C NMR (126 MHz, $CDCl_3$): δ = 156.1 (C^{A2}), 149.1 (C^{A6}), 142.2 (C^{B4}), 134.4 (d, J_{PC} = 14 Hz, $C^{B2/3}$), 134.2 (C^{A4}), 130.1 (d, J_{PC} = 12 Hz, $C^{B2/3}$), 126.9 (d, J_{PC} = 59 Hz, C^{B1}), 126.5 (C^{A5}), 124.4 (C^{A3}), 21.7 (C^{Me}) (C≡C signals not observed) ppm. ^{31}P NMR (162 MHz, $CDCl_3$): δ = 40.6 (s) ppm. UV/Vis (CH_2Cl_2): λ_{max} (ε) = 239 (100500), 253 sh (88000), 269 (69000), 286 (71000), 303 (28000), 315 (21000 $dm^3 mol^{-1} cm^{-1}$) nm; emission (CH_2Cl_2, λ_{exc} = 285 nm): λ_{max} = 338, 438, 466 nm. ESI-MS (CH_2Cl_2): m/z = 805.2 $[Au\{(4\text{-Tol})_3P\}_2]^+$ (calcd. 805.2), 1205.1 $[M + H]^+$ (calcd. 1205.3), 1705.0 $[M + AuP(4\text{-Tol})_3]^+$ (calcd. 1705.4). $C_{56}H_{48}Au_2N_2P_2 \cdot Et_2O \cdot H_2O$ (1297.01): calcd. C 55.56, H 4.66, N 2.16; found C 55.67, H 4.54, N 2.12.

Compound 3: Et_3PAuCl (68.7 mg, 196 μmol), 4,4′-diethynyl-2,2′-bipyridine (20 mg, 98 μmol) and CuI (0.2 mg, 1 μmol). Compound **3** was isolated as white solid (25.6 mg, 30.8 μmol, 31.4%). ^1H NMR (500 MHz, $CDCl_3$): δ = 8.50 (dd, J = 5.0, 0.8 Hz, 2 H, H^{A6}), 8.33 (dd, J = 1.4, 0.8 Hz, 2 H, H^{A3}), 7.27 (dd, J = 5.0, 1.6 Hz, 2 H, H^{A5}), 1.81 (dq, J_{PH} = 9.6, J_{HH} = 7.7 Hz, 12 H, H^{CH_2}), 1.20 (dt, J_{PH} = 18.1, J_{HH} = 7.6 Hz, 18 H, H^{CH_3}) ppm. ^{13}C NMR (126 MHz, $CDCl_3$): δ = 156.1 (C^{A2}), 149.1 (C^{A6}), 134.2 (C^{A4}), 126.4 (C^{A5}), 124.4 (C^{A3}), 18.0 (d, J_{PC} = 33 Hz, C^{CH_2}), 9.1 (C^{CH_3}) (C≡C signals not observed) ppm. ^{31}P NMR (162 MHz, $CDCl_3$): δ = 39.1 (s) ppm. UV/Vis (CH_2Cl_2): λ_{max} (ε) = 236 (49000), 267 (55000), 284 (60500), 303 (23000), 316 (19000 $dm^3 mol^{-1} cm^{-1}$) nm; emission (CH_2Cl_2, λ_{exc} = 284 nm): λ_{max} = 350, 438, 466 nm. ESI-MS (CH_2Cl_2): m/z = 433.3 $[Au(PEt_3)_2]^+$ (calcd. 433.2), 833.3 $[M + H]^+$ (calcd. 833.2), 1147.1 $[M + AuPEt_3]^+$ (calcd. 1147.2). $C_{26}H_{36}Au_2N_2P_2$ (832.46): calcd. C 37.51, H 4.36, N 3.37; found C 37.48, H 4.19, N 3.16.

Compound 4: iPr_3PAuCl (76.9 mg, 196 μmol), 4,4′-diethynyl-2,2′-bipyridine (20 mg, 98 μmol) and CuI (0.2 mg, 1 μmol). Compound **4** was isolated as white solid (36.4 mg, 39.7 μmol, 40.5%). ^1H NMR (500 MHz, $CDCl_3$): δ = 8.49 (d, J = 5.0 Hz, 2 H, H^{A6}), 8.35 (s, 2 H, H^{A3}), 7.27 (dd, J = 5.0, 1.5 Hz, 2 H, H^{A5}), 2.29 (m, 6 H, $H^{iPr\text{-}CH}$), 1.33 (dd, J_{PH} = 15.5, J_{HH} = 7.2 Hz, 36 H, H^{CH_3}) ppm. ^{13}C NMR (126 MHz, $CDCl_3$): δ = 156.0 (C^{A2}), 149.1 (C^{A6}), 134.3

(C^{A4}), 126.3 (C^{A5}), 124.4 (C^{A3}), 23.9 (d, J_{PC} = 28 Hz, $C^{iPr\text{-}CH}$), 20.5 (C^{CH_3}) (C≡C signals not observed) ppm. ^{31}P NMR (162 MHz, $CDCl_3$): δ = 67.6 (s) ppm. UV/Vis (CH_2Cl_2): λ_{max} (ε) = 236 (57000), 267 (63000), 283 (69000), 303 (28000), 315 (21000 $dm^3 mol^{-1} cm^{-1}$) nm; emission (CH_2Cl_2, λ_{exc} = 284 nm): λ_{max} = 348, 438, 464 nm. ESI-MS (CH_2Cl_2): *m*/*z* = 517.4 $[Au(PiPr_3)_2]^+$ (calcd. 517.2), 917.4 $[M + H]^+$ (calcd. 917.3), 1173.2 $[M + AuPEt_3]^+$ (calcd. 1173.4). $C_{32}H_{48}Au_2N_2P_2$ (916.62): calcd. C 41.93, H 5.28, N 3.06; found C 42.13, H 5.21, N 2.85.

X-ray Crystallography: Data were collected with a Bruker-Nonius Kappa CCD or Stoe IPDS instrument; data reduction, solution and refinement used the programs COLLECT,[57] SIR92,[58] DENZO/SCALEPACK[59] and CRYSTALS,[60] or Stoe IPDS software[61] and SHELXL97.[62] Structures were analysed by using Mercury v. 2.2.[17]

2{1}·Et$_2$O: $C_{104}H_{82}Au_4N_4OP_4$, M = 2315.58, colourless needle, triclinic, space group $P\bar{1}$, a = 9.5773(7), b = 13.021(1), c = 17.913(1) Å, α = 104.278(4), β = 90.541(4), γ = 92.994(4)°, V = 2161.4(3) Å^3, Z = 1, $D_{calcd.}$ = 1.779 Mg m^{-3}, μ(Mo-K_α) = 6.894 mm^{-1}, T = 173 K, 46687 reflections collected (14247 unique), merging r = 0.061. Refinement of 8213 reflections (550 parameters) with $I > 3.0\sigma(I)$ converged at final $R1$ = 0.0474 [$R1$(all data) = 0.0904], $wR2$ = 0.0393 [$wR2$(all data) = 0.0449], gof = 1.0433.

2·Et$_2$O: $C_{60}H_{58}Au_2N_2OP_2$, M = 1279.01, colourless prism, triclinic, space group $P\bar{1}$, a = 9.2636(7), b = 10.3025(7), c = 13.691(1) Å, α = 94.056(4), β = 97.201(4), γ = 92.625(4)°, V = 1291.1(2) Å^3, Z = 1, $D_{calcd.}$ = 1.645 Mg m^{-3}, μ(Mo-K_α) = 5.779 mm^{-1}, T = 123 K, 84925 reflections collected (17279 unique), merging r = 0.032. Refinement of 14073 reflections (322 parameters) with $I > 3.0\sigma(I)$ converged at final $R1$ = 0.0236 [$R1$(all data) = 0.0327], $wR2$ = 0.0224 [$wR2$(all data) = 0.0291], gof = 1.0467.

3: $C_{26}H_{36}Au_2N_2P_2$, M = 832.47, colourless needle, monoclinic, space group $P2_1/c$, a = 14.5466(4), b = 14.5575(4), c = 12.9700(4) Å, β = 96.508(2)°, V = 2728.9(1) Å^3, Z = 4, $D_{calcd.}$ = 2.026 Mg m^{-3}, μ(Mo-K_α) = 10.8874 mm^{-1}, T = 123 K, 119769 reflections collected (15011 unique), merging r = 0.047. Refinement of 9322 reflections (289 parameters) with $I > 3.0\sigma(I)$ converged at final $R1$ = 0.0187 [$R1$(all data) = 0.0427], $wR2$ = 0.0198 [$wR2$(all data) = 0.0315], gof = 1.0559.

4: $C_{32}H_{48}Au_2N_2P_2$, M = 916.60, colourless plate, orthorhombic, space group *Pbcn*, a = 13.571(3), b = 15.069(3), c = 16.309(3) Å, V = 3335.3(12) Å^3, Z = 4, $D_{calcd.}$ = 1.825 Mg m^{-3}, μ(Mo-K_α) = 8.906 mm^{-1}, T = 173(2) K, 102936 reflections collected (3104 unique), merging r = 0.2171. Refinement of 3061 reflections (199 parameters) with $I > 2.0\sigma(I)$ converged at final $R1$ = 0.0677 [$R1$(all data) = 0.0681], $wR2$ = 0.01790 [$wR2$(all data) = 0.1796], gof = 1.243.

CCDC-739607 (2{**1**}·Et$_2$O), -739604 (**2**·Et$_2$O), -739605 (**3**) and -739606 (**4**) contain the supplementary crystallographic data for this paper. These data can be obtained free of charge from The Cambridge Crystallographic Data Centre via www.ccdc.cam.ac.uk/data_request/cif.

Acknowledgments

We thank the University of Basel and the Swiss National Science Foundation for financial support. Kate Harris and Dr. Valerie Jullien are thanked for recording 500 MHz NMR spectra.

[1] H. Schmidbaur, A. Schier in *Comprehensive Organometallic Chemistry III* (Eds.: R. H. Crabtree, D. M. P. Mingos), Elsevier, Oxford, **2007**, vol. 2, chapter 5, p. 251–307.
[2] N. J. Long, C. K. Williams, *Angew. Chem. Int. Ed.* **2003**, *42*, 2586–2617.
[3] C.-M. Che, S.-W. Lai in *Gold Chemistry* (Ed.: F. Mohr), Wiley-VCH, Weinheim, **2009**, p. 249–281.
[4] V. W.-W. Yam, C.-L. Chan, C.-K. Li, K. M.-C. Wong, *Coord. Chem. Rev.* **2001**, *216–217*, 173–194.
[5] V. W.-W. Yam, E. C.-C. Cheng, *Chem. Soc. Rev.* **2008**, *37*, 1806–1813.
[6] V. W.-W. Yam, E. C.-C. Cheng, *Top. Curr. Chem.* **2007**, *281*, 269–309.
[7] V. W.-W. Yam, *Acc. Chem. Res.* **2002**, *35*, 555–563.
[8] D. Li, X. Hong, C. M. Che, W. C. Lo, S. M. Peng, *J. Chem. Soc., Dalton Trans.* **1993**, 2929–2932.
[9] P. Li, B. Ahrens, K.-H. Choi, M. S. Khan, P. R. Raithby, P. J. Wilson, W.-Y. Wong, *CrystEngComm* **2002**, *4*, 405–412, and references therein.
[10] C.-M. Che, H.-L. Kwong, V. W.-W. Yam, K.-C. Cho, *J. Chem. Soc., Chem. Commun.* **1989**, 885–886.
[11] C. King, J.-C. Wang, M. N. I. Khan, J. P. Fackler Jr, *Inorg. Chem.* **1989**, *28*, 2145–2149.
[12] R. J. Puddephatt, *Coord. Chem. Rev.* **2001**, *216–217*, 313–332.
[13] H. Schmidbaur, *Gold Bull.* **1990**, *23*, 11–21.
[14] H. Schmidbaur, *Chem. Soc. Rev.* **1995**, *24*, 391–400.
[15] P. Pyykkö, *Angew. Chem. Int. Ed.* **2004**, *43*, 4412–4456.
[16] H. Schmidbaur, A. Schier, *Chem. Soc. Rev.* **2008**, *37*, 1931–1951.
[17] I. J. Bruno, J. C. Cole, P. R. Edgington, M. K. Kessler, C. F. Macrae, P. McCabe, J. Pearson, R. Taylor, *Acta Crystallogr., Sect. B* **2002**, *58*, 389–397.
[18] R.-L. Liau, A. Schier, H. Schmidbaur, *Organometallics* **2003**, *22*, 3199–3204.
[19] E. C. Constable, C. E. Housecroft, M. Neuburger, S. Schaffner, E. J. Shardlow, *Dalton Trans.* **2007**, 2631–2633.
[20] C. P. McArdle, M. J. Irwin, M. C. Jennings, R. J. Puddephatt, *Angew. Chem. Int. Ed.* **1999**, *38*, 3376–3378.
[21] F. Mohr, D. J. Eisler, C. P. McArdie, K. Atieh, M. C. Jennings, R. J. Puddephatt, *J. Organomet. Chem.* **2003**, *670*, 27–36.
[22] F. Mohr, M. C. Jennings, R. J. Puddephatt, *Eur. J. Inorg. Chem.* **2003**, 217–223.
[23] C. P. McArdle, M. J. Irwin, M. C. Jennings, J. J. Vital, R. J. Puddephatt, *Chem. Eur. J.* **2002**, *8*, 723–734.
[24] M. J. Irwin, J. J. Vital, R. J. Puddephatt, *Organometallics* **1997**, *16*, 3541–3547.
[25] S.-J. Shieh, X. Hong, S.-M. Peng, C.-M. Che, *J. Chem. Soc., Dalton Trans.* **1994**, 3067–3068.
[26] I. R. Whittall, M. G. Humphrey, S. Houbrechts, J. Maes, A. Persoons, S. Schmid, D. C. R. Hockless, *J. Organomet. Chem.* **1997**, *544*, 277–283.
[27] M. A. MacDonald, R. J. Puddephatt, G. P. A. Yapp, *Organometallics* **2000**, *19*, 2194–2199.
[28] J. Vicente, M.-T. Chicote, M. M. Alvarez-Falcon, D. Bautista, *Organometallics* **2004**, *23*, 5707–5712.
[29] N. C. Habermehl, M. C. Jennings, C. P. McArdle, F. Mohr, R. J. Puddephatt, *Organometallics* **2005**, *24*, 5004–5014.
[30] J. Vicente, J. Gil-Rubio, N. Barquero, P. G. Jones, D. Bautista, *Organometallics* **2008**, *27*, 646–659.
[31] M. Ferrer, A. Gutierrez, L. Rodriguez, O. Rossell, J. C. Lima, M. Font-Bardia, X. Solans, *Eur. J. Inorg. Chem.* **2008**, 2899–2909.
[32] H.-B. Xu, L.-Y. Zhang, J. Ni, H.-Y. Chao, Z.-N. Chen, *Inorg. Chem.* **2008**, *47*, 10744–10752.
[33] E. C. Constable, C. E. Housecroft, M. Neuburger, S. Schaffner, E. J. Shardlow, *Polyhedron* **2008**, *27*, 65–70.
[34] P. Li, B. Ahrens, A. D. Bond, J. E. Davies, O. F. Koentjoro, P. R. Raithby, S. J. Teat, *Dalton Trans.* **2008**, 1635–1646.
[35] N. C. Habermehl, F. Mohr, D. J. Eisler, M. C. Jennings, R. J. Puddephatt, *Can. J. Chem.* **2006**, *84*, 111–123.
[36] R. Packheiser, A. Jakob, P. Ecorchard, B. Walfort, H. Lang, *Organometallics* **2008**, *27*, 1214–1226.

[37] R. Packheiser, P. Ecorchard, T. Ruffer, B. Walfort, H. Lang, *Eur. J. Inorg. Chem.* **2008**, 4152–4165.
[38] H.-Y. Ye, F.-R. Dai, Z.-N. Chen, *Acta Crystallogr., Sect. E* **2007**, *63*, m1576–m1576.
[39] See for example: B.-C. Tzeng, A. Schier, H. Schmidbaur, *Inorg. Chem.* **1999**, *38*, 3978–3984.
[40] X. He, E. C.-C. Cheng, N. Zhu, V. W.-W. Yam, *Chem. Commun.* **2009**, 4016–4018.
[41] P. Pyykkö, P. Zaleski-Ejgierd, *J. Chem. Phys.* **2008**, *128*, 124309/1–124309/6.
[42] R. Ziessel, J. Suffert, M. T. Youinou, *J. Org. Chem.* **1996**, *61*, 6535–6546.
[43] M. I. Bruce, M. Jevric, B. W. Skelton, M. E. Smith, A. H. White, N. N. Zaitseva, *J. Organomet. Chem.* **2006**, *691*, 361–370.
[44] G. Desiraju, *Acc. Chem. Res.* **2002**, *35*, 565–573.
[45] G. Desiraju, *Chem. Commun.* **2005**, 2995–3001.
[46] G. Desiraju, T. Steiner, *The Weak Hydrogen Bond*, Oxford University Press, Oxford, **1999**.
[47] T. Steiner, *Angew. Chem. Int. Ed.* **2002**, *41*, 48–76.
[48] M. Nishio, M. Hirota, Y. Umezawa, *The C–H···π Interaction: Evidence, Nature and Consquences*, Wiley, Weinheim, **1998**.
[49] M. Nishio, *CrystEngComm* **2004**, *41*, 130–158.
[50] C. A. Tolman, *Chem. Rev.* **1977**, *77*, 313–348.
[51] T. Mutai, J.-D. Cheon, G. Tsuchiya, K. Araki, *J. Chem. Soc. Perkin Trans. 2* **2002**, 862–865.
[52] H. H. Jaffé, L. D. Freedman, *J. Am. Chem. Soc.* **1952**, *74*, 1069–1071.
[53] V. W.-W. Yam, S. W.-K. Choi, K.-K. Cheung, *Organometallics* **1996**, *15*, 1734–1739.
[54] V. W.-W. Yam, S. W.-K. Choi, *J. Chem. Soc., Dalton Trans.* **1996**, 4227–4232.
[55] Y. Bao, C. Zhong, D. M. Vu, J. P. Temirov, R. B. Dyer, J. S. Martinez, *J. Phys. Chem. C* **2007**, *111*, 12194–12198.
[56] M. I. Bruce, E. Horn, J. G. Matisons, M. R. Snow, *Aust. J. Chem.* **1984**, *37*, 1163–1170.
[57] *COLLECT Software*, Nonius BV, **1997–2001**.
[58] A. Altomare, G. Cascarano, G. Giacovazzo, A. Guagliardi, M. C. Burla, G. Polidori, M. Camalli, *J. Appl. Crystallogr.* **1994**, *27*, 435–435.
[59] Z. Otwinowski, W. Minor, *Methods in Enzymology* (Eds.: C. W. Carte Jr, R. M. Sweet), Academic Press, New York, **1997**, vol. 276, pp. 307.
[60] P. W. Betteridge, J. R. Carruthers, R. I. Cooper, K. Prout, D. J. Watkin, *J. Appl. Crystallogr.* **2003**, *36*, 1487–1487.
[61] *IPDS Software*, version 1.26, Stoe & Cie, Darmstadt, Germany, **1996**.
[62] G. M. Sheldrick, *Acta Crystallogr., Sect. A* **2008**, *64*, 112–122.

Received: July 29, 2009
Published Online: September 22, 2009

